Permafrost Characteristics along Trail Ridge Road, Rocky Mountain National Park, CO

Jason Janke
Metropolitan State College of Denver
Department of Earth and Atmospheric Sciences, CB 22
Denver, CO 80217

Report provided for the following project.

Rocky Mountains Cooperative Ecosystem Studies Unit (RM-CESU)
RM-CESU Cooperative Agreement Number: H12000040001

TITLE OF PROJECT: Field Investigation of Permafrost Distribution along Trail Ridge Road, Rocky Mountain National Park, CO

NAME OF PARK/NPS UNIT: Rocky Mountain National Park

NAME OF UNIVERSITY PARTNER: University of Colorado at Boulder

NPS KEY OFFICIAL: Cheri Yost, Park Ranger, Rocky Mountain National Park, 1000 Highway 36, Estes Park, CO 80517, phone: 970-586-1394, cheri_yost@nps.gov

PRINCIPAL INVESTIGATOR: Jason Janke, Institute of Arctic and Alpine Research
University of Colorado, Campus Box 450, Boulder, CO 80309-0450, phone: 303-556-3072, Jason.Janke@colorado.edu

COST OF PROJECT:

Direct Cost: $ 9,117

Indirect Cost (CESU overhead): $ 1,595

Total Cost: $ 10,712

NPS ACCOUNT NUMBER: 1526-0006-RZZ

NAME OF FUND SOURCE: ONPS ROMO base funds

Introduction

Permafrost, or ground that remains at or below 0° C for at least two consecutive years, has been modeled using a variety Geographic Information Systems (GIS) techniques (Ives and Fahey 1971; Ives 1974; Janke 2005a). Janke (2005b) showed that a 2.0–2.5°C temperature increase could dramatically reduce permafrost extent by about 95% in the Front Range of Colorado. Several sections of Trail Ridge Road (TRR) could potentially be affected by future warming. As the ground warms, localized slumping, loss of soil cohesion from melting ice, or regional subsidence could pose a threat (Isaken et al. 2007; Lantz and Kokelj 2008). Direct temperature measurements of soil could provide a valuable method to map permafrost and monitor long-term temperature and environmental conditions along TRR. The objectives of this study are to: 1) provide a detailed account of the permafrost distribution along TRR and 2) better understand the effect of environmental variables (elevation, aspect, slope, soil texture, etc.) on ground temperature measurements.

Study Area

The study area extends 6 miles (9.7 km) along a gently sloping (2 to 25°) periglacial surface (Figure 1). Within the study area, elevations range from 12,080 ft (3,682 m) on the eastern side of TRR to 11,539 ft (3,517 m) on the western side. The highest point along TRR rests at 12,182 ft (3,713 m). The road is exposed to a variety of aspects; southern and western facing slopes are common as the road parallels the Big Thompson River, but northwestern facing slopes are more common as the road veers north. Alpine tundra borders most sections of the road, although certain sections cut through bedrock and talus accumulations. Earth hummocks, perennial snow patches, patterned ground, rock wedges, stone stripes, and solifluction lobes are all present.

Methods

As part of the project, Metropolitan State College of Denver undergraduate students who have limited exposure to scientific research served as field and lab assistants (Figure 2). This provided an authentic, applied learning opportunity for underrepresented and underserved

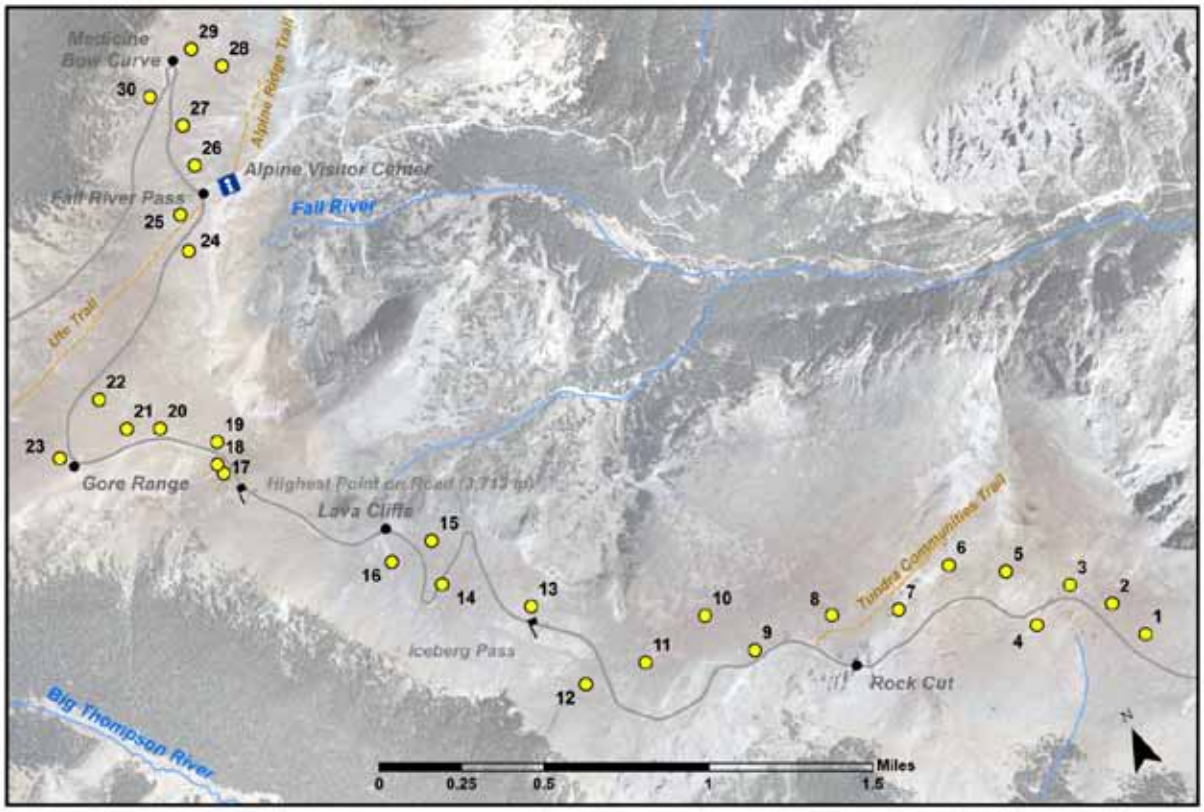

Figure 1 – Location of 30 sample points along TRR in Rocky Mountain National Park. (Back)

Figure 2 – A) A student using a soil auger to install a data logger; B) students attempting to relocate a data logger during the fall; C) students analyzing nutrient concentrations in the lab; D) students examining soil properties; E) field assistants installing a data logger on a stone stripe; F) Dr. Janke explaining the project to his field studies class; and G) a field assistant attempting to drill deeper into the tundra. (Back)

students. Thirty HOBO data loggers with two sensors (internal (A) and an external (B)) were installed during July 2008 (Figure 3). With the assistance of students, holes were drilled using a standard soil auger, sensors were inserted, and holes were backfilled. Unfortunately, the rocky soil did not permit the second sensor to be placed at a great depth. Internal surface sensors (A) were installed at 10 cm depth, whereas external sensor (B) depths ranged from 30 to 85 cm. Soil samples were obtained at each site for analysis of soil properties. For each sensor location, elevation, slope, and aspect were measured (Table 1). Loggers were launched and set to record temperature at 2-hour intervals. High-resolution Global Positioning Satellite (GPS) measurements were taken at each point to aid in relocation. Locations were also marked with a ring of rocks around the data logger.

Soils were analyzed for the following nutrients: nitrogen, phosphorous, potassium, calcium, magnesium, and sulfur. Conductivity (µS/cm), a measure of the soil's salt concentration, and pH were also measured for each location. Bulk Density (g/cm³), a measure of the mass of a soil (including pore spaces) in relation to its volume, particle density (g/cm³), a measure of the mass of just the soil particles in relation to the volume, and porosity (%), a measure of the void spaces in a soil, were measured in order to determine their potential relationship with ground temperature measurements.

During July 2009, loggers were relocated and data were downloaded. Only 4 of 60 (7%) sensors contained errors in their readings. Averages, standard deviations, maximums, and minimums were calculated for each sensor. In order to determine potential indicators of permafrost, subsets of the data were used to calculate averages and standard deviations for the winter months (December through February). The frost index, an indicator of permafrost presence, was calculated using the following formula:

$$FI = \frac{\sqrt{Frozen\ \ Days}}{[\sqrt{Thawed\ \ Days} + |\sqrt{Frozen\ \ Days}|]} \qquad (1)$$

Depth to permafrost was estimated for each point. This formula is based on an estimate of the thermal conductivity of the soil. The warmest summer months were averaged in order to provide a conservative estimate of the possible depth to permafrost. The distance between the

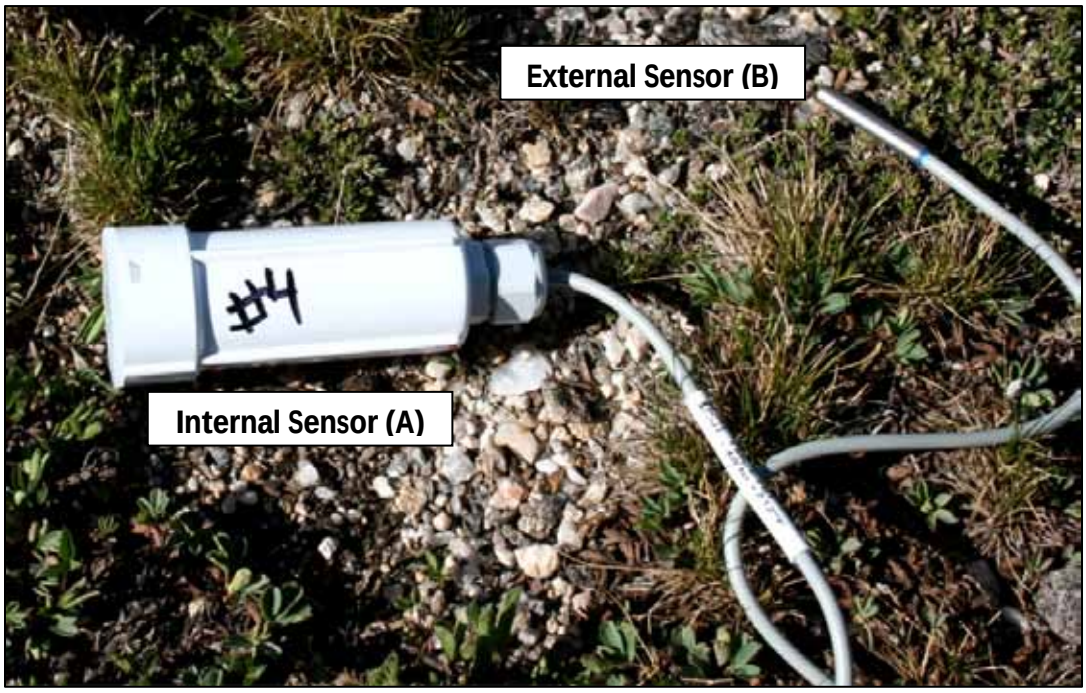

Figure 3 – Example of a HOBO internal/external temperature data logger. (Back)

Table 1 – Environmental characteristics of the selected field sites. (Back)

Point	Site Description	Aspect (Direction)	Elevation (m)	Slope (°)
1	Rock wedge	SW	3688	19
2	Side of solifluction lobe	WSW	3690	15
3	Earth hummock	SSW	3684	4
4	Tundra	SE	3677	14
5	Tundra	NE	3707	13
6	Downslope from snowpack	SSE	3724	12
7	Tundra below rock outcrop	SE	3736	17
8	Center of rock wedge	NW	3711	7
9	Tundra	W	3685	7
10	Solifluction step	N	3651	12
11	Center of rock wedge	NNW	3647	8
12	Tundra	W	3607	19
13	Wet slump	NE	3614	14
14	Frost heaving	SE	3665	8
15	Tundra with stone stripes	E	3678	13
16	Exposed tundra surface	SSE	3692	2
17	In between stone stripes	W	3702	25
18	Coarse rock	W	3700	24
19	Tundra	SW	3733	19
20	Stone stripes	SW	3720	10
21	Tundra	W	3699	6
22	Active heave	N	3675	15
23	Tundra	NW	3658	10
24	Rocky mixture in tundra	NNW	3625	23
25	Rocky mixture in tundra	NW	3580	17
26	Tundra	WNW	3604	13
27	Disturbed soil	NW	3590	18
28	Stone stripes	N	3603	18
29	Bog-sedge-alder	N	3565	10
30	Tundra	NW	3530	17

surface and the bottom temperature probe was calculated. This formula assumes a linear temperature decrease with depth between the 2 points, which is unrealistic in nature. An exponential function would likely be realistic; however, only two vertical temperature measurements locations per point did not permit an exponential calculation. Therefore, the uncertainty associated with this calculation is high.

$$Depth\ to\ Permafrost = \frac{A}{[(A-B)/Distance\ \ between\ \ Points\ ]}, \text{ where} \qquad (2)$$

A = June – September average at A (10 cm) and

B = June – Sept. average at B (30 – 85 cm).

Results and Discussion

Soil Properties

Soil properties for each sample are summarized in Table 2. Figure 4 and Figure 5 provide examples of nutrient concentrations across the study area as well as variations in conductivity, pH, bulk density, particle density, and porosity. Concentration of nutrients generally decrease with depth. This is consistent with other soil types as well since nutrients stored in vegetation are broken down and added to the soil surface. Calcium is the most abundant plant nutrient in the tundra soils followed by sulfur. In plants, calcium is required to act as a "bouncer," regulating the intake of other nutrients and is important for nodule formation and root growth. Sulfur is needed as a plant protein. Magnesium and potassium have lower concentrations. Magnesium is needed for photosynthesis, and potassium helps create stuff stems and plump grains. Phosphorous and nitrogen, two of the most important plant nutrients because of their ability to increase biomass, productivity, root formation, and make plants more winter hardy, have the lowest concentration in the alpine soils (Table 2). Most soils had a slightly acidic pH (5 on average), which may be the result of acid precipitation, particularly accumulations of snow that are acidic in nature. Bulk densities averaged about 1.12 g/cm^3, and porosity averaged about 48%, a typical value for a silt to clay loam soil (Table 2).

Table 2 – Soil characteristics for sample points. (Back)

Point	Nitrogen (lb/acre)	Phosphorous (lb/acre)	Potassium (lb/acre)	Calcium (lb/acre)	Magnesium (lb/acre)	Sulfur (lb/acre)	Conductivity (µS/cm)	pH	Bulk Density (g/cm³)	Particle Density (g/cm³)	Porosity (%)
1A	--	--	--	--	--	--	--	--	--	--	--
1B	3	90	280	--	--	--	--	5.0	0.85	1.40	61
2A	2	120	240	--	--	--	--	5.0	1.02	1.40	73
2B	--	--	--	--	--	--	--	5.0	1.25	2.65	47
3A	3	75	200	700	10	100	120	4.0	0.61	1.40	44
3B	3	150	180	700	10	500	136	4.2	0.53	1.40	38
4A	40	50	25	1400	20	100	113	4.5	1.31	2.65	49
4B	10	50	100	1400	10	500	103	4.5	1.15	2.65	43
5A	25	200	100	150	100	25	210	5.5	0.56	1.40	40
5B	2	120	100	350	300	60	177	6.0	1.36	2.65	51
6A	3	200	300	2800	50	4000	128	6.0	1.45	2.65	55
6B	3	200	280	2000	50	500	125	5.0	1.05	2.65	40
7A	40	25	180	2800	50	100	183	4.6	0.40	1.40	29
7B	10	10	100	700	5	500	63	4.5	1.34	2.65	51
8A	20	150	180	2800	50	100	218	5.0	0.73	1.40	52
8B	20	25	140	2800	20	500	320	5.0	0.99	2.65	37
9A	20	75	400	2000	10	100	365	4.5	0.51	1.40	36
9B	10	25	160	2000	10	100	135	4.5	1.62	2.65	61
10A	4	150	210	2800	600	20	1113	5.7	0.66	1.40	47
10B	100	150	100	150	100	25	480	5.8	1.05	2.65	40
11A	--	--	--	--	--	--	--	5.4	0.48	1.40	34
11B	3	60	400	350	680	250	223	6.5	1.18	2.65	45
12A	100	150	400	350	700	60	380	5.7	0.64	1.40	46
12B	6	85	300	1000	740	40	364	6.2	0.90	2.65	34
13A	5	90	400	2000	20	400	152	5.2	0.52	2.65	20
13B	3	75	300	2000	50	400	105	4.7	1.38	2.65	52
14A	2	130	600	150	800	25	182	6.8	1.30	2.65	49
14B	8	105	800	150	360	20	152	5.8	1.40	2.65	53
15A	3	100	220	2800	20	400	135	5.0	1.40	2.65	53
15B	3	75	300	2000	20	400	133	4.5	1.75	2.65	66
16A	2	100	140	151	423	40	204	4.2	0.81	1.40	58
16B	1	25	100	155	516	60	97	4.3	1.21	2.65	46
17A	--	--	--	--	--	--	--	5.0	1.07	2.65	40
17B	--	--	--	--	--	--	--	4.0	1.07	2.65	40
18A	--	--	--	--	--	--	--	--	--	--	--
18B	--	--	--	--	--	--	--	5.0	1.53	2.65	58
19A	100	150	100	350	300	70	229	5.7	0.66	1.40	47
19B	3	10	160	760	700	300	700	5.9	1.03	1.40	74
20A	150	10	110	700	50	100	89	4.5	1.64	2.65	62
20B	60	10	100	2000	10	200	110	5.5	1.66	2.65	63
21A	3	20	100	140	139	16	130	4.7	1.19	2.65	45
21B	3	25	140	167	65	6	343	4.6	1.35	2.65	51
22A	11	150	100	330	854	8	0	5.0	1.50	2.65	57
22B	7	150	90	371	643	8	--	4.0	1.60	2.65	60
23A	15	150	100	371	582	8	0	4.8	0.58	1.40	41
23B	10	80	200	371	272	8	--	4.4	1.36	2.65	51
24A	3	50	380	123	150	100	134	4.1	0.97	2.65	37
24B	3	75	140	878	82	60	102	4.5	1.40	2.65	53
25A	3	10	130	493	45	100	191	5.8	1.31	2.65	49
25B	4	10	100	833	86	200	125	5.1	1.41	2.65	53
26A	--	--	--	--	--	--	--	4.4	1.03	2.65	39
26B	--	--	--	--	--	--	--	4.8	1.41	2.65	53
27A	5	150	400	2000	300	40	134	4.7	1.75	2.65	66
27B	5	90	400	700	160	16	100	5.0	1.24	2.65	47
28A	23	25	400	350	300	20	313	4.5	0.95	2.65	36
28B	--	--	--	--	--	--	--	5.0	1.30	2.65	49
29A	150	10	160	2000	10	2000	224	4.2	1.02	1.40	73
29B	20	10	130	2000	20	100	129	4.6	1.30	2.65	49
30A	3	10	250	2800	50	400	166	5.4	1.02	2.65	38
30B	3	100	300	2800	50	2000	120	5.8	1.36	2.65	51

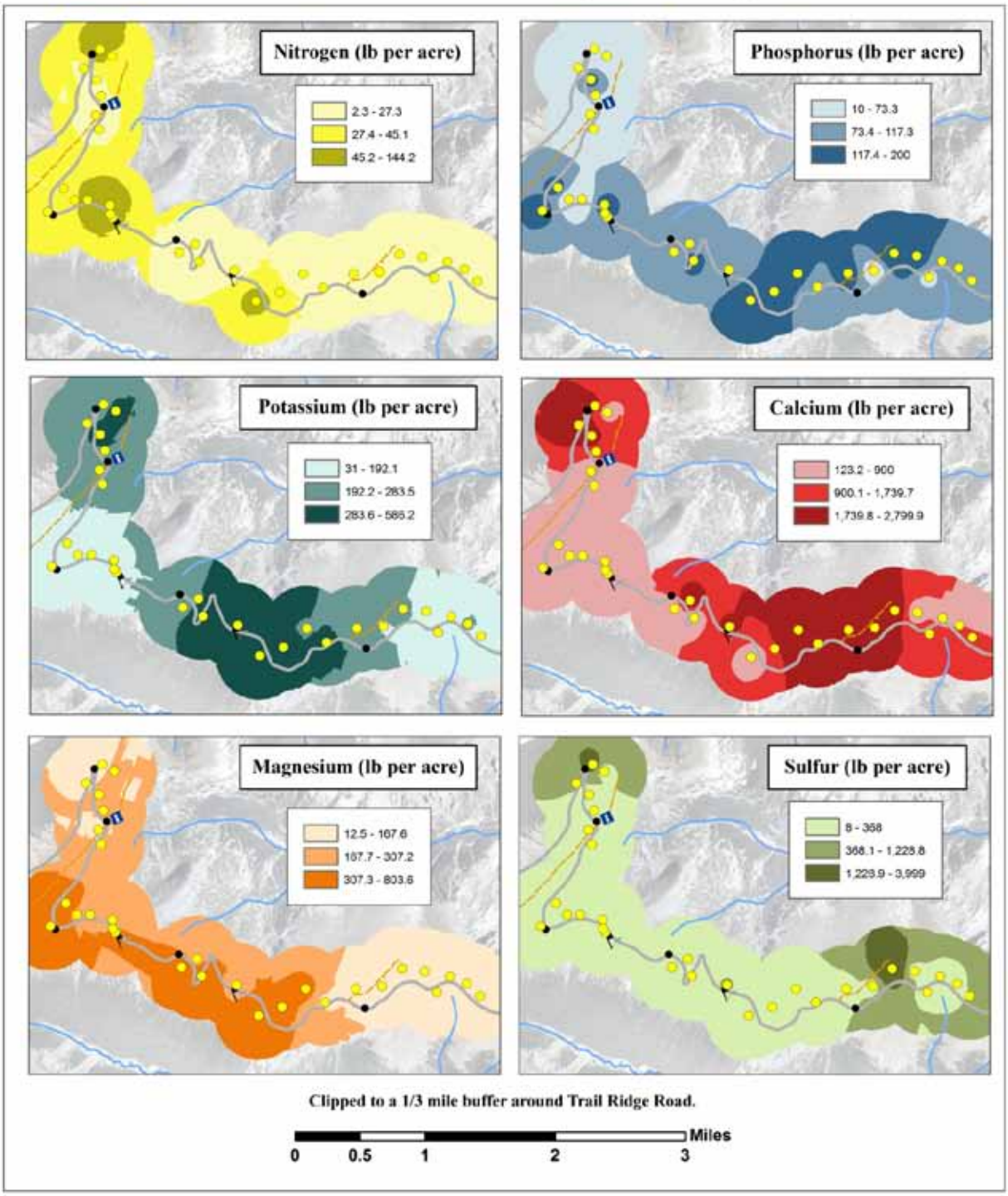

Figure 4 – Nitrogen, Phosphorus, Potassium, Calcium, Magnesium, and Sulfur concentrations for soils along Trail Ridge Road. (Back)

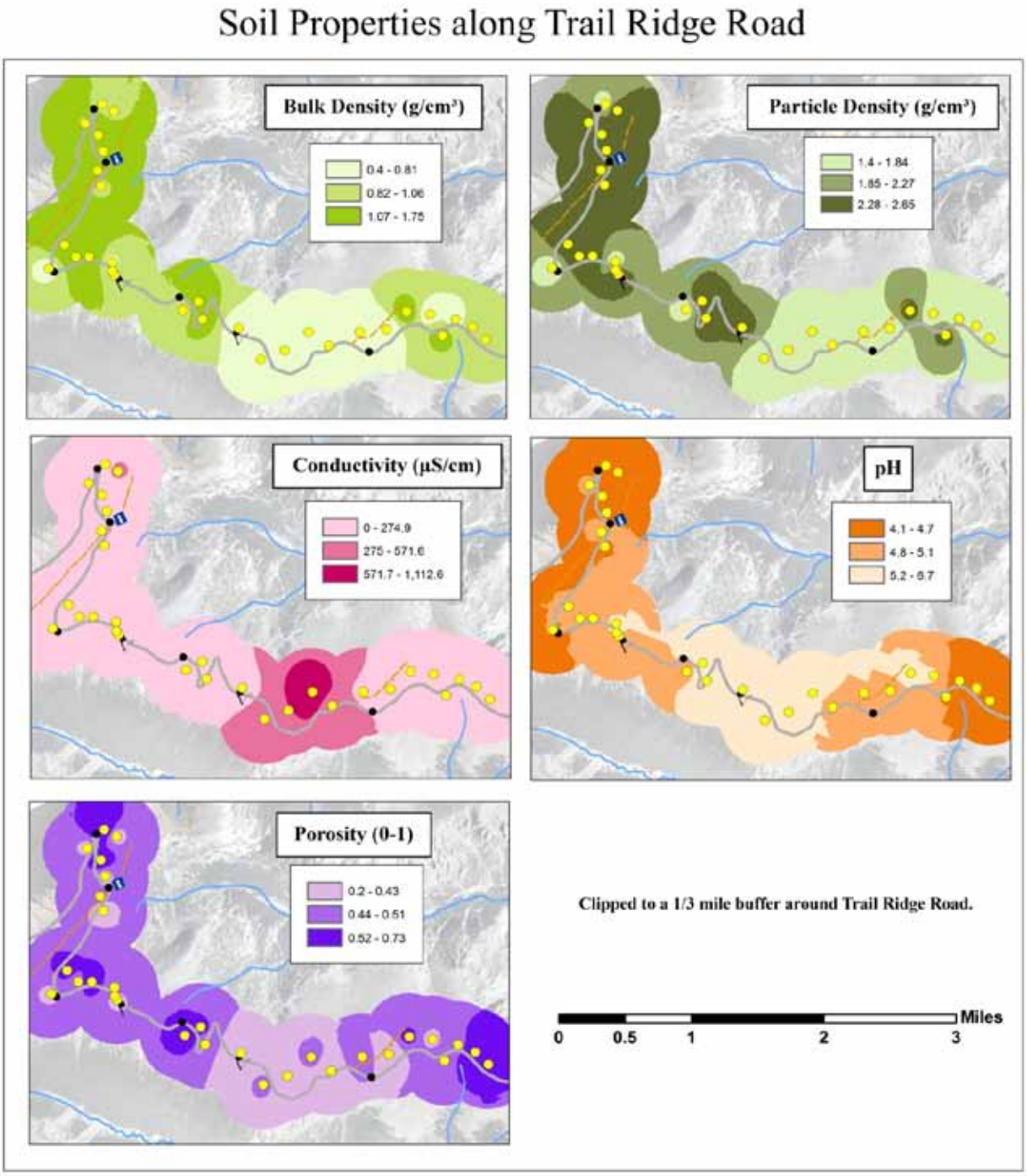

Figure 5 – Selected soil properties along Trail Ridge Road. (Back)

Soil Temperature

Soil temperatures measurements are listed in Table 3. A maximum temperature of 26.1 °C (79.0 °F) and a minimum temperature of -17.8 °C (0.0 °F) were observed for all samples. Minimum and maximum temperatures occurred at the surface for the majority of sites, indicating greater variability in surface temperature measurements compared to those at depth (Figure 6). The mean annual soil temperature for all sites was -1.1 °C (30.0 °F). In general, soil temperatures were colder on the western side of the study area at high elevations (Figure 7; Figure 8). Means were similar for the surface (A) and deeper probes (B); however, the standard deviation was greater at the surface compared to at depth (Table 3). This illustrates the dampening effect of the soil as it acts as an insulator to resist temperature change on both a seasonal and daily (diurnal) scale. Variation during the course of a day is greater in the summer months compared to the winter months. Snow covers some sites during the winter months, acts as an insulator, and reduces extreme temperature variation. Maximum temperatures occurred in mid-July to early August, whereas minimum temperatures were recorded at the end of December for most sites. These data suggest that direct solar radiation, snow cover, and air temperature are important variables that influence daily and seasonal alpine soil temperatures.

Winter month means (Dec. – Feb.) were -7.0 °C (19.4 °F). As a rule-of-thumb applied to the European Alps, Hoelzle et al. (1993) suggested that a Bottom Temperature of winter Snow (BTS) below -3.0 °C (26.6 °F) indicates the presence of permafrost at depth (Figure 9). According to this rule, all 30 sites should have permafrost; however, this model was designed for the European Alps, which vary considerably in terms of topography and climate compared to the Rocky Mountains. In the future, borehole drillings are perhaps the best method to acknowledge the presence of permafrost with greater certainty at some of these locations. Once permafrost existence is validated, a similar rule-of-thumb could be developed for the Rocky Mountains.

Based on Equation 1, an average frost index of 0.56 was calculated for all sites. Frost indexes ranged from 0.51 to 0.60 (Figure 10). These values are typical for sporadic permafrost

Table 3 – Temperature data for sample points. (Back)

Point	Depth (cm)	Maximum (°C)	Maximum Date	Minimum (°C)	Minimum Date	Mean Temperature (°C)	Standard Deviation (°C)	Dec. to Feb. Mean (°C)	Dec. to Feb. Standard Deviation (°C)	Depth to Permafrost (m)	Frost Index
1A	10	26.1	7/19/2008	-17.6	12/21/2008	-1.5	7.7	-9.2	2.5	1.1	0.58
1B	30	9.9	8/1/2008	-10.1	12/21/2008	-1.5	5.1	-7.1	1.5	1.1	0.58
2A	10	13.8	7/19/2008	-13.8	12/21/2008	-1.4	6.2	-8.5	2.1	1.8	0.55
2B	80	6.4	7/14/2008	-7.6	2/21/2009	-1.2	3.8	-5.1	1.8	1.8	0.55
3A	10	13.6	7/31/2008	-8.7	1/5/2009	0.1	4.5	-4.3	1.3	1.4	0.58
3B	30	7.7	8/9/2008	-5.7	1/5/2009	0.0	3.3	-3.1	1.0	1.4	0.58
4A	10	19.7	7/19/2008	-13.7	12/21/2008	-0.8	6.1	-6.5	2.4	2.0	0.58
4B	30	10.6	8/1/2008	-8.0	1/7/2009	-0.6	4.8	-5.1	1.9	2.0	0.56
5A	10	15.7	7/31/2008	-14.7	12/21/2008	-1.2	7.0	-9.1	2.1	2.7	0.55
5B	35	9.5	8/2/2008	-10.5	12/21/2008	-1.1	5.9	-7.8	1.6	2.7	0.54
6A	10	20.5	8/30/2008	-12.8	12/27/2008	-0.9	7.1	-7.9	2.7	2.5	0.55
6B	50	9.9	8/2/2008	-8.7	2/20/2009	-0.7	5.4	-5.8	2.2	2.5	0.51
7A	10	14.0	8/1/2008	-11.9	12/21/2008	-1.0	6.3	-8.2	1.8	2.2	0.55
7B	65	7.2	8/3/2008	-7.6	2/21/2009	-0.9	4.6	-5.7	1.6	2.2	0.54
8A	10	11.9	7/31/2008	-14.1	12/27/2008	-2.3	6.2	-9.2	2.0	--	0.58
8B	45	--	--	--	--	--	--	--	--	--	--
9A	10	19.8	8/1/2008	-15.2	12/21/2008	-1.1	7.0	-9.1	2.3	--	0.54
9B	30	--	--	--	--	--	--	--	--	--	--
10A	10	16.8	7/5/2008	-10.2	1/6/2009	-0.9	5.5	-5.9	1.5	1.9	0.60
10B	70	8.3	7/13/2008	-3.7	3/15/2009	-0.8	3.5	-3.7	1.1	1.9	0.58
11A	10	13.1	8/1/2008	-9.2	12/21/2008	-0.4	4.9	-5.2	1.5	1.9	0.58
11B	75	6.4	7/14/2008	-5.1	3/13/2009	-0.3	3.1	-2.8	1.4	1.9	0.57
12A	10	13.9	7/19/2008	-13.4	12/21/2008	-1.0	6.3	-7.8	1.7	3.3	0.55
12B	30	9.2	7/26/2008	-11.7	12/21/2008	-1.1	5.6	-7.8	1.7	3.3	0.54
13A	10	21.1	7/9/2008	-1.8	4/3/2009	1.2	3.5	-0.6	0.4	--	0.56
13B	75	5.0	9/1/2008	-1.0	2/14/2009	0.7	1.7	0.0	0.1	--	--
14A	10	17.9	7/31/2008	-17.4	12/22/2008	-1.3	7.2	-9.3	2.9	2.7	0.55
14B	85	7.7	8/3/2008	-8.1	2/21/2009	-0.8	4.7	-5.9	1.8	2.7	0.55
15A	10	17.9	7/31/2008	-15.1	12/21/2008	-1.1	6.8	-8.6	2.3	--	0.56
15B	40	--	--	--	--	--	--	--	--	--	--
16A	10	17.4	7/31/2008	-16.0	12/27/2008	-1.3	6.6	-8.8	2.6	1.9	0.55
16B	45	7.9	8/2/2008	-9.5	12/28/2008	-1.1	4.8	-6.6	1.6	1.9	0.54
17A	10	14.7	7/19/2008	-14.8	12/21/2008	-2.0	6.4	-9.0	2.3	1.3	0.55
17B	55	5.7	7/27/2008	-10.1	12/28/2008	-2.3	4.6	-7.1	2.2	1.3	0.58
18A	10	9.7	8/1/2008	-13.7	12/21/2008	-2.5	5.5	-8.3	2.5	2.2	0.59
18B	85	5.4	8/3/2008	-9.0	2/22/2009	-2.1	4.1	-5.6	2.6	2.2	0.60
19A	10	15.9	7/31/2008	-17.1	12/21/2008	-1.8	7.0	-9.4	2.8	3.0	0.55
19B	35	11.2	7/17/2008	-13.3	12/21/2008	-1.5	6.2	-8.3	2.3	3.0	0.53
20A	10	19.6	7/19/2008	-17.8	12/21/2008	-1.4	7.5	-10.0	2.9	3.3	0.54
20B	40	12.0	7/20/2008	-12.6	12/28/2008	-1.1	6.3	-8.6	2.0	3.3	0.54
21A	10	14.6	7/31/2008	-13.3	3/14/2009	-1.7	6.5	-8.9	1.9	3.2	0.56
21B	30	9.7	7/19/2008	-11.5	3/14/2009	-1.7	5.9	-8.2	1.7	3.2	0.56
22A	10	16.6	7/19/2008	-14.6	12/21/2008	-1.9	6.2	-8.4	1.8	2.0	0.59
22B	70	7.5	8/3/2008	-7.7	1/7/2009	-1.8	4.3	-6.1	1.4	2.0	0.60
23A	10	14.7	7/19/2008	-10.7	12/21/2008	-1.1	5.6	-7.3	1.4	1.3	0.58
23B	50	6.4	7/14/2008	-6.8	2/22/2009	-1.2	3.8	-5.2	1.3	1.3	0.58
24A	10	19.6	7/19/2008	-16.7	12/21/2008	-1.4	7.2	-9.6	2.3	2.2	0.55
24B	40	9.1	8/2/2008	-11.1	12/21/2008	-1.4	5.7	-8.0	1.5	2.2	0.54
25A	10	22.7	8/1/2008	-16.9	12/21/2008	-1.2	7.2	-8.7	2.3	2.2	0.55
25B	60	9.0	8/2/2008	-8.3	2/22/2009	-1.0	4.9	-6.1	1.3	2.2	0.55
26A	10	17.2	7/19/2008	-12.2	12/21/2008	-0.5	6.1	-7.4	1.7	2.0	0.54
26B	40	7.6	8/2/2008	-8.0	12/21/2008	-0.6	4.7	-6.1	1.3	2.0	0.52
27A	10	19.0	7/19/2008	-16.2	12/21/2008	-1.4	7.0	-9.2	2.3	2.0	0.56
27B	55	8.6	8/1/2008	-8.9	12/25/2008	-1.2	4.9	-6.5	1.4	2.0	0.55
28A	10	16.8	7/19/2008	-14.4	12/21/2008	-1.8	6.5	-8.5	1.8	2.4	0.59
28B	30	11.2	8/1/2008	-10.7	12/25/2008	-1.7	5.6	-7.6	1.4	2.4	0.59
29A	10	12.9	7/19/2008	-8.6	12/20/2008	-1.0	4.5	-5.5	2.0	--	0.55
29B	50	--	--	--	--	--	--	--	--	--	--
30A	10	12.5	7/25/2008	-11.6	12/21/2008	-0.9	5.6	-7.7	1.7	2.0	0.54
30B	50	6.4	7/27/2008	-7.5	2/21/2009	-0.9	4.4	-5.7	1.3	2.0	0.53

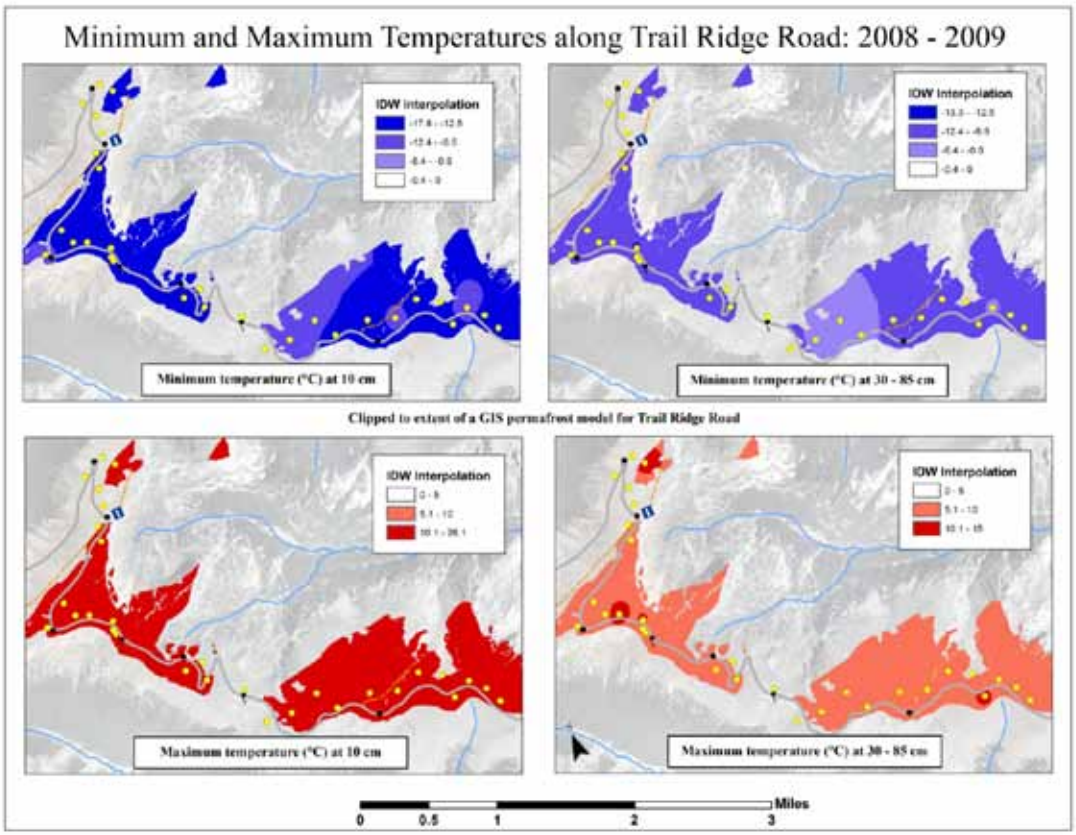

Figure 6 – Minimum and maximum temperatures along Trail Ridge Road. (Back)

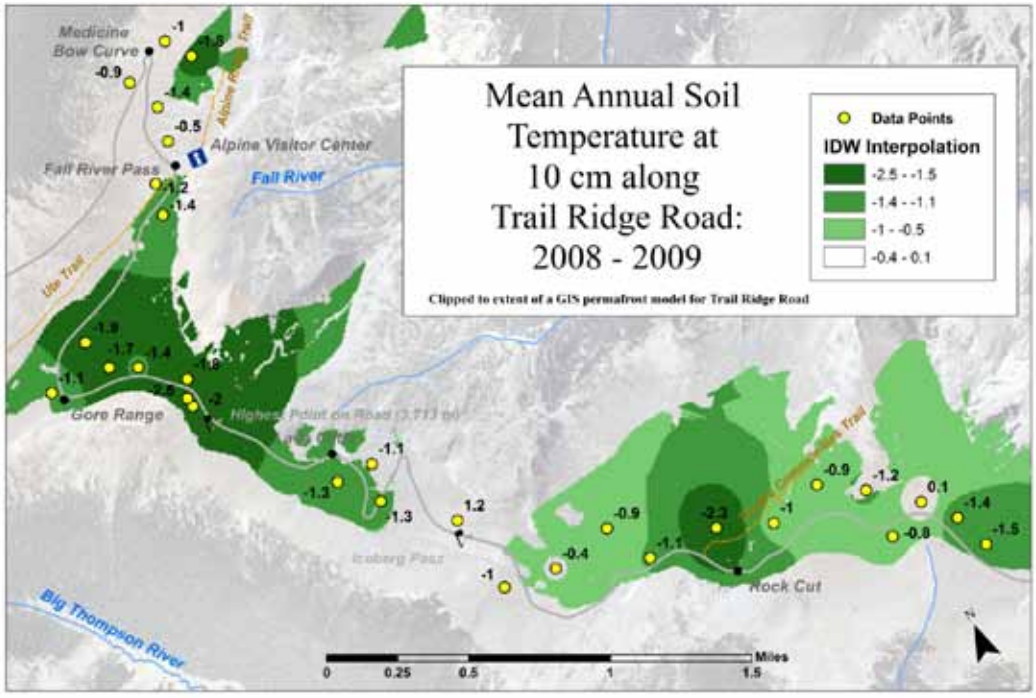

Figure 7 – Mean Annual Soil Temperature at the surface. (Back)

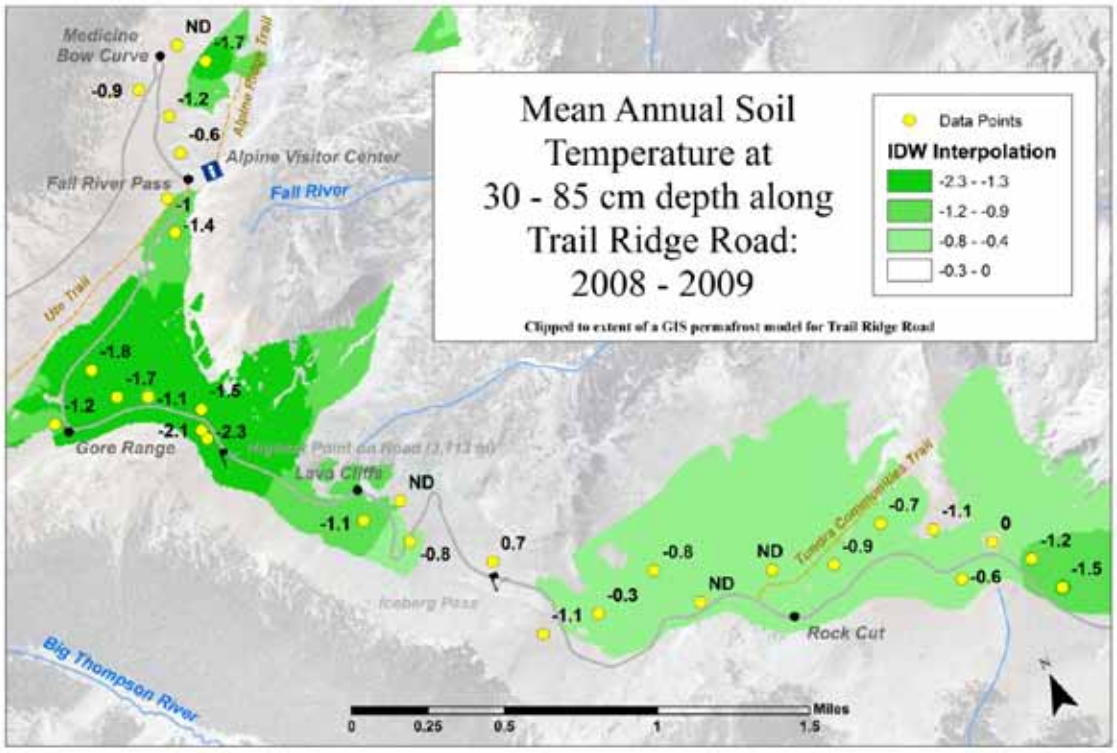

Figure 8 - Mean Annual Soil Temperature at depth. (Back)

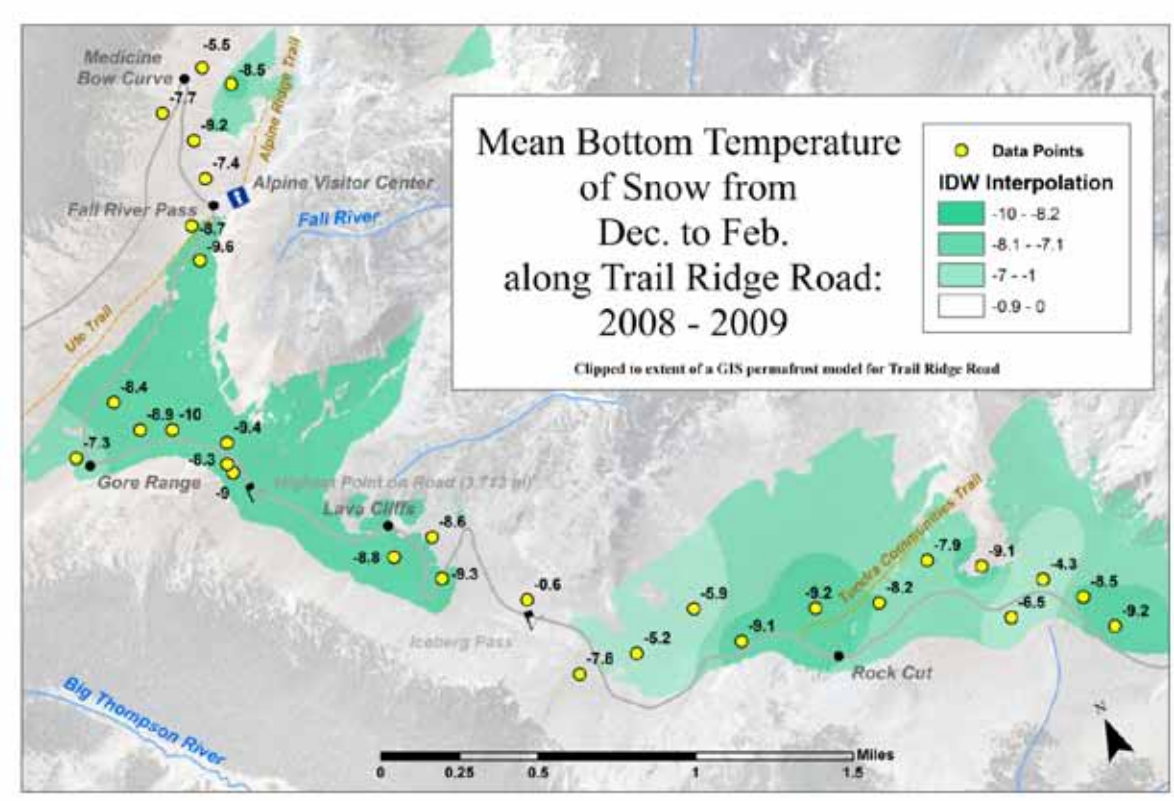

Figure 9 – Bottom Temperature of Winter Snow along Trail Ridge Road. (Back)

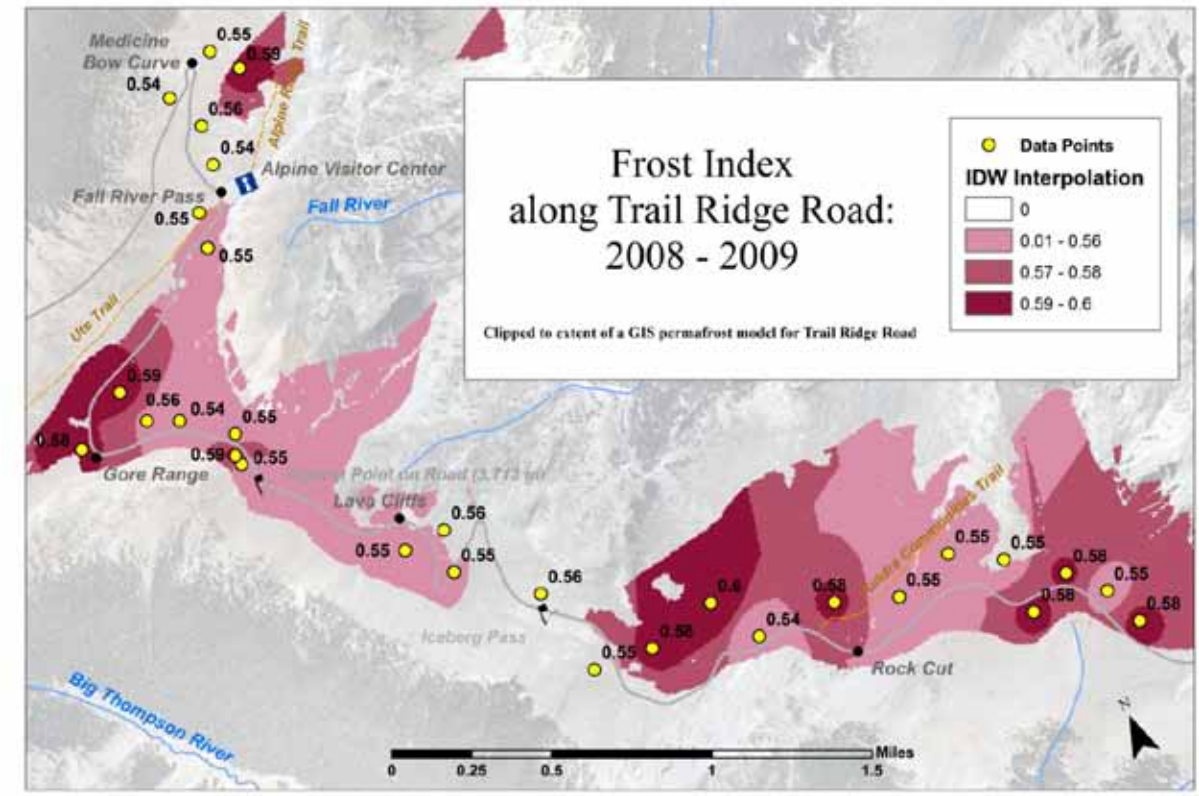

Figure 10 – Frost Indexes along Trail Ridge Road. (Back)

and indicate that the soil is frozen at all sites for the majority of days (> 183 days) during a year. Frost indexes were used to model the probability of permafrost occurrence. Frost indexes greater than 0.56 were considered an indicator of probable permafrost, whereas frost indexes of 0.55 were considered an indicator of possible permafrost. Elevation and aspect were measured for each site and were plotted on a polar diagram (Figure 11). The study area was then classified using a GIS model based on the probable and possible categories (Figure 12). Northern facing slopes should have the greatest frost indexes since they receive less solar radiation; however, this was not the case. Interestingly, western facing slopes had a higher occurrence of permafrost based on the frost indexes. This may be the result of limited samples on northern facing slopes. Another explanation may be related to minimal snow cover and therefore less insulation at these sites; ideal locations for permafrost lack snow cover. Snow cover as thin as 25 – 50 cm can warm ground (Williams and Smith 1989). The western facing periglacial slopes may be windswept and are exposed to harsh winter air temperatures.

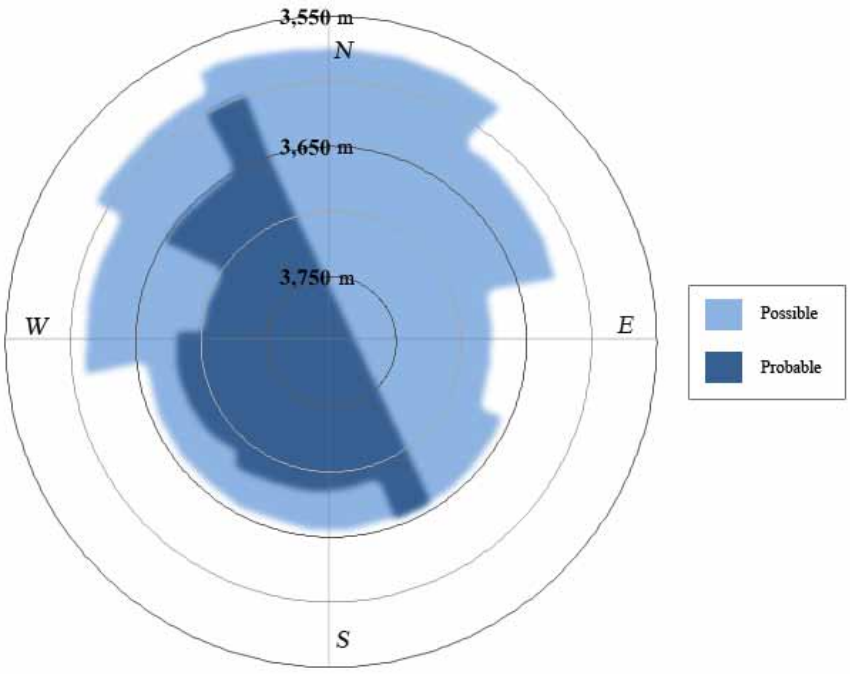

Figure 11 – Polar diagram for probable and possible permafrost. (Back)

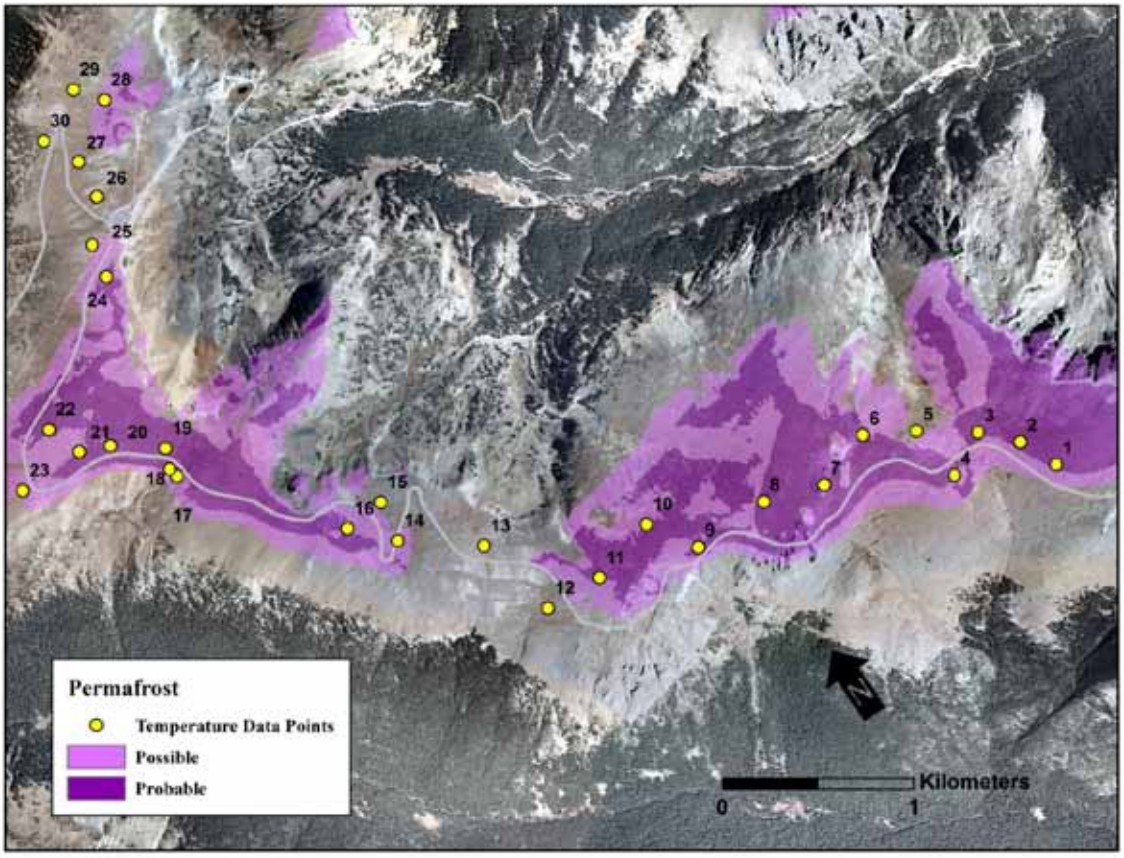

Figure 12 – Probable and possible permafrost along Trail Ridge Road. (Back)

Average depth to permafrost was 2.2 m using Equation 2. Depths to permafrost were greater on the northern side of the study area, past the highest elevation on TRR (Figure 13). Similar active layer thicknesses (≈ 2 – 3 m) were obtained for nearby Niwot Ridge, CO using geophysical estimates (Leopold et al. 2008).

Relationship between Soil Temperatures and Environmental Variables

Mean annual soil temperature (MAST) data were compared with elevation, aspect, and slope through a simple correlation analysis (Figure 14). Correlations were generally weak (greatest $R^2 = 0.30$); however, slope exhibited the strongest relationship with MAST. Steeper slopes had lower MAST. This may be related to snow distribution, as less snow is likely to accumulate and therefore insulate steep slopes. Aspect exhibited the second strongest correlation ($R^2 = 0.16$) suggesting that western and northern slopes have lower MAST. The strength of this correlation could be improved if ranges of aspects from additional sample sites are examined. Elevation displayed the weakest correlation with MAST ($R^2 < 0.08$). MAST only showed a slight decrease when higher elevations were reached. A range of only about 200 m was examined which may not be large enough to illustrate the effect of elevation on temperature. The relationship between MAST and soil texture (bulk density, particle density, and porosity) was non-existent. Porosity could affect permafrost formation by two means. First, soils with low porosities (sands) should have greater thermal conductivities; greater porosities (clays) should have lower thermal conductivities. Greater thermal conductivity is advantageous for permafrost formation because it allows cold air to penetrate deeply into the soil. Second, greater porosities lead to greater potential for water storage. Soils with greater moisture content should have greater thermal conductivities (by as much as 10 times) compared to dry soils. Ice content increases the thermal conductivity more so compared to water. Soil properties showed no correlation with MAST. The complex interaction of these open-system variables is too difficult to decipher in the field setting; perhaps individual variables could be manipulated more effectively in a closed-system laboratory experiment.

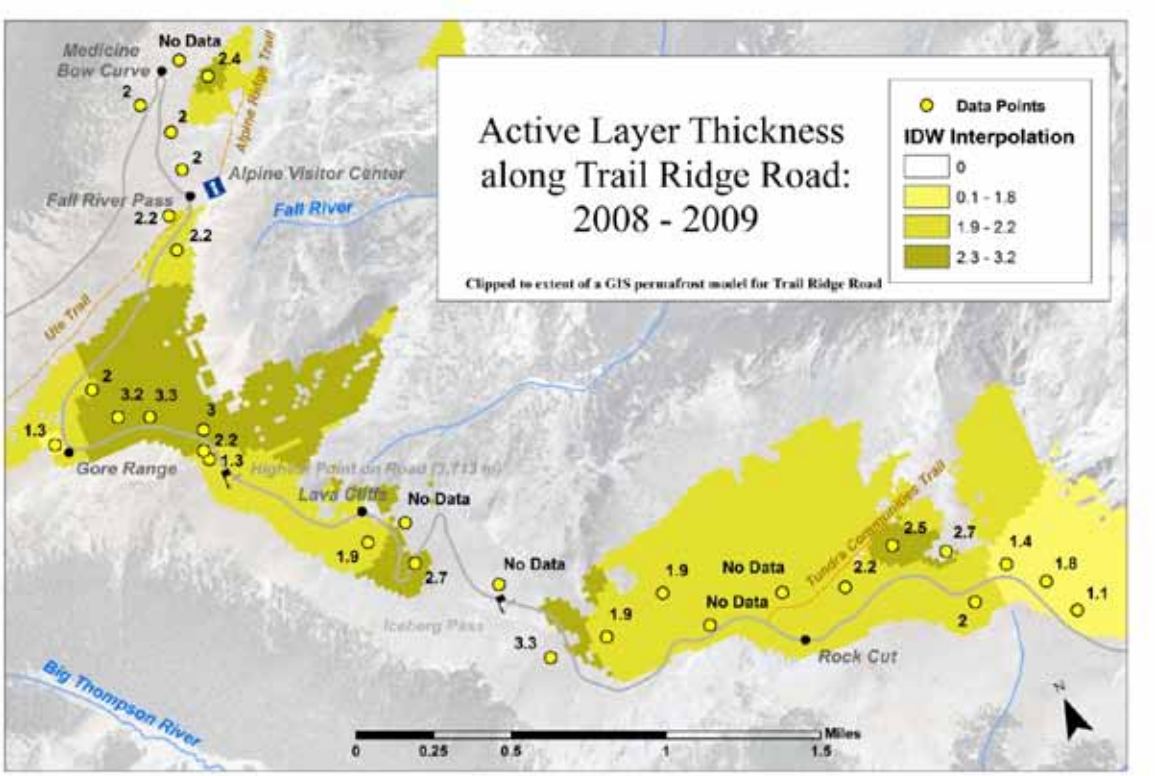

Figure 13 – Depth to permafrost along Trail Ridge Road. (Back)

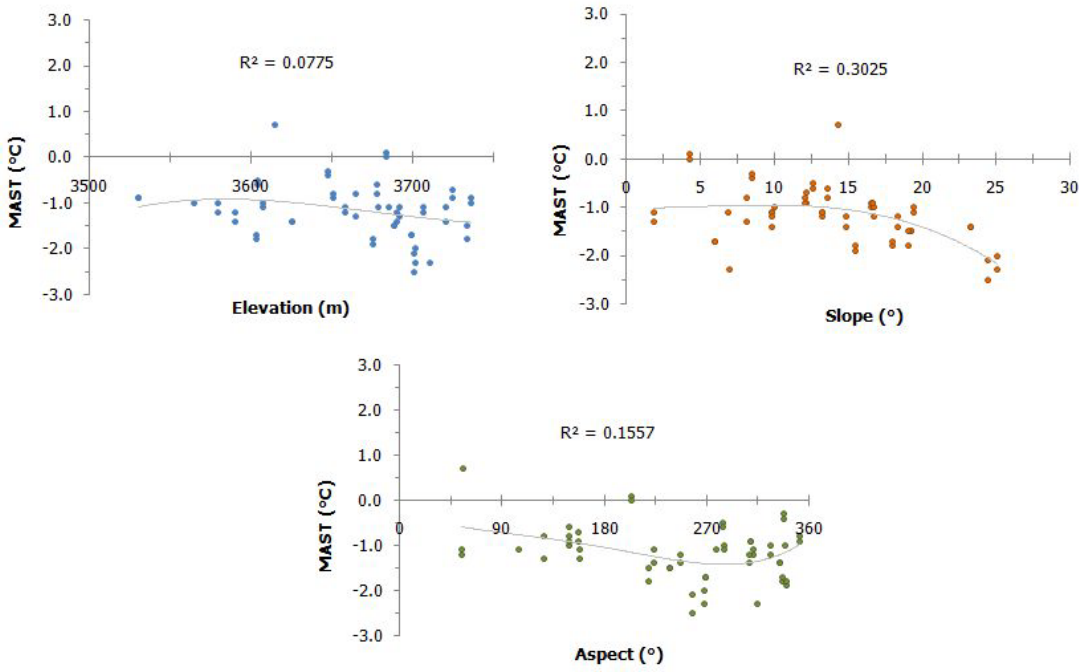

Figure 14 – Relationship among Mean Annual Soil Temperature (MAST), Elevation, Slope, and Aspect. (Back)

Sites with Unique Signatures

Four sites exhibit unique thermal signatures that indicate permafrost presence (Figure 15). During December to mid-May, soil water is frozen as temperatures remain below 0 °C. Thaw begins in the late spring. As the thawing front advances from the surface, latent heat is absorbed due to a phase change from ice to water. As a result, temperatures remain steady at slightly below 0 °C from mid-May until mid-June. Ground temperatures rise quickly through July and stabilize in August. The energy balance becomes negative in fall and the soil begins to freeze from the surface through mid-October. Large quantities of latent heat are released through a phase change from water to ice. This opposes the cooling, and temperatures reach equilibrium from mid-October through December. This effect is often referred to as the zero curtain, which has a unique isothermal plateau signature and is strongly correlated with the occurrence of permafrost. Freezing fronts from the surface and at depth advance toward each other and freeze the active layer from each direction. Eventually, the stability disappears after large quantities of latent heat are removed and temperatures steeply drop through the winter (Outcalt and Hinkel 1996, Boike et al. 2008).

Three other sites were chosen to illustrate the effect of ground cover on temperature. Site 1 rests on an accumulation of rock that is bordered by tundra. Site 3 is located on an earth hummock that has organic soils, and Site 6 rests below a perennial snow patch. Compared to other locations, Site 1 has a greater standard deviation, but overall cold temperatures (Figure 16). Balch ventilation, in which void spaces between coarse rocks funnel colder air, is likely responsible for the variation and overall cooler average temperatures (Haeberli 1985). Site 3 has a MAST close to 0 °C. In comparison to the other sites, it is warmer but has a smaller variance and still remains frozen for the majority of the year as indicated by a high Frost Index value of 0.58 (Figure 16). This site provides a good example of the stabilizing effects that organic soil or peat content have on soil temperatures. Peat has a high thermal conductivity to keep it cold during the winter, but also has the capability to store water during the summer. Evaporation of water absorbs latent heat, keeping the organic soil cooler than normal during the summer (Williams and Smith 1989). At Site 6, a spring snowmelt signature exists. At the

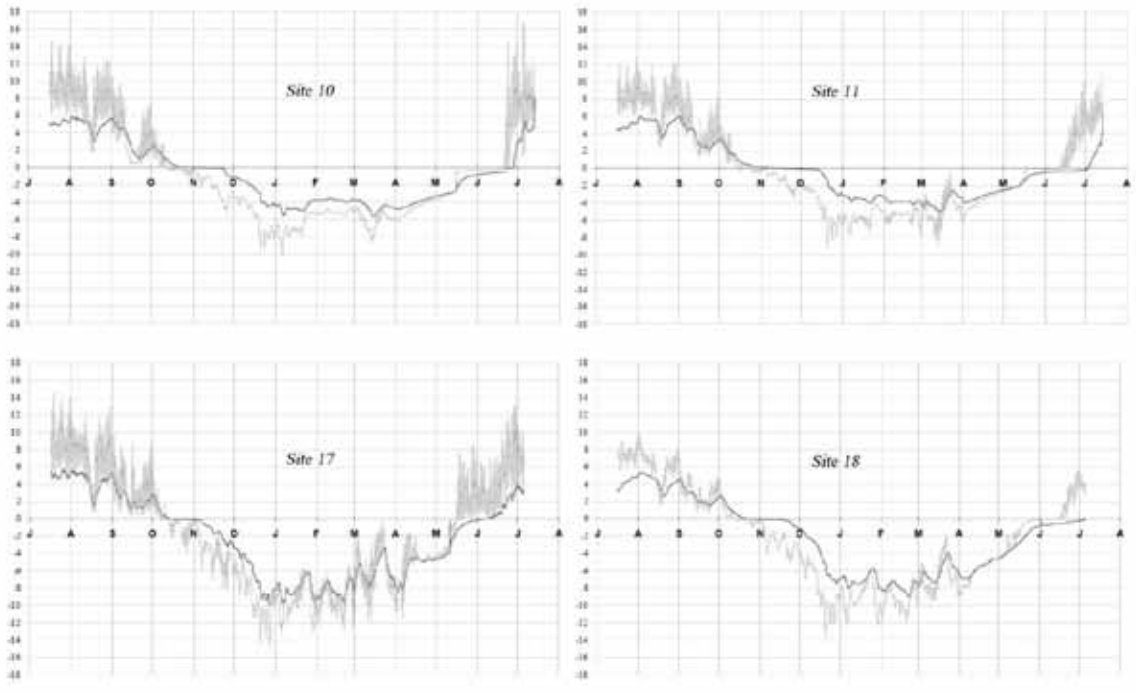

Figure 15 – Zero curtain signatures for sites 10, 11, 17, and 18 that indicate the presence of probable permafrost. (Back)

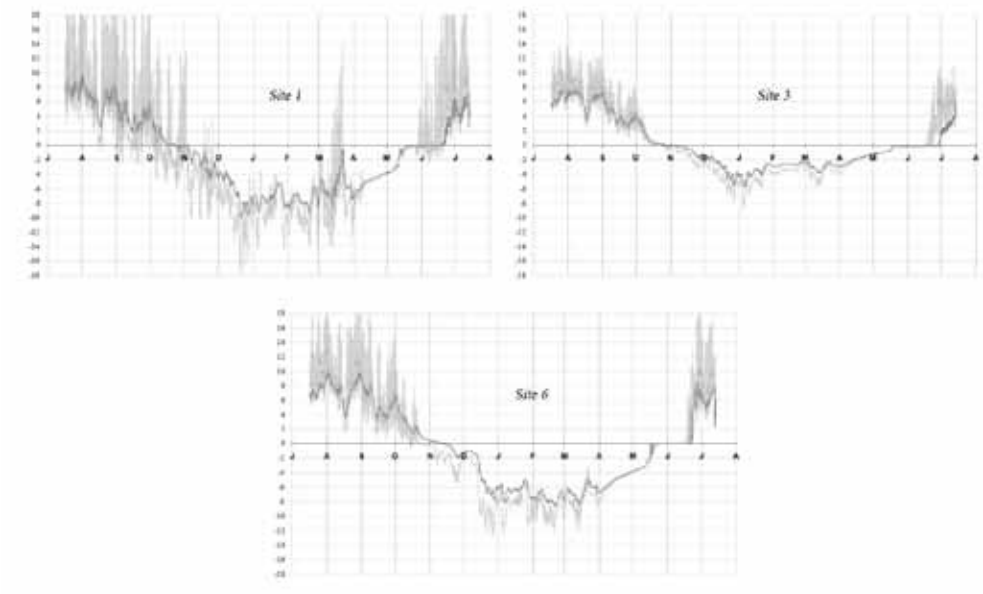

Figure 16 – The effects of ground cover on temperature measurements for rock (Site 1), organic soil (Site 3), and below a snow patch (Site 6). Dark lines are deep probes, whereas light grey lines are surface probes. (Back)

deep probe, the temperature is constant at 0 °C during an extended period after the near surface probe goes above 0 °C (Figure 16). This likely indicates the drainage of snowmelt along a "wet line" that halts at the frozen surface of the active layer.

Conclusions

Soil temperatures along TRR remain frozen for the majority of the year. In fact, only 2 of 30 sites had an average temperature greater than 0 °C at the surface. Elevation, aspect, and slope all exhibited weak correlations with MAST. The strongest correlation was between slope and MAST; sites with colder temperatures tended to have steeper slopes, suggesting that limited snow accumulation may enhance permafrost formation.

For all sites, winter month means (Dec. – Feb.) were -7.0 °C (19.4 °F). According to the European definition of permafrost based on BTS, all 30 sites would likely contain some form of permafrost. A more conservative estimate of permafrost was established using Frost Indexes and GIS modeling techniques (Figure 10). Permafrost likely underlies a 1.5 mile (2.4 km) stretch of TRR from Point 1 to Point 11. Near Iceberg Pass, permafrost ceases to exist. Another section of permafrost is likely to exist along a 2.5 mile (4.0 km) section of TRR ranging from Point 14 to Point 25 (Figure 11). Permafrost is likely to be discontinuous and sporadic. According to temperature signatures that stabilize at or near 0 °C during the fall due to permafrost releasing latent heat (the zero curtain effect), Points 10, 11, 17, and 18 are most likely to contain permafrost (Figure 14). These sites should be considered for borehole drillings to verify the presence of permafrost.

Recommended Areas of Study

In the future, soil temperatures should continue to be monitored to detect possible warming of alpine soils. Comparisons should also be made with other measurements from nearby locations, such as those sensors in the Green Lakes Valley, CO or the Never Summer Range to verify a long-term, regional signal. Measurements from exposed ridges, alpine peaks, or valleys that experience cold air drainage will provide a better understanding of the topographic effects on Rocky Mountain microclimates. Snow surveys should also be conducted

to understand the interaction of the timing, depth, and duration of snow and the associated effects on soil temperature. If a correlation exists, a visual surface variable as simple as limited or thin snow distribution could be used to indicate highly probable areas of permafrost occurrence at a regional scale. Geophysical methods such as Ground Penetrating Radar or Electrical Conductivity methods could help provide a better approximation of the spatial variability of permafrost along TRR. These non-obstructive 2-D and 3-D methods cover a larger region along transects compared to isolated sample points used in this study (Vonder Mühll 2002; Hauck and Vonder Mühll 2003). Geophysical methods could also be used temporally to monitor permafrost evolution over yearly periods or over the course of seasons (Riseborough et al. 2008; Schott and Sass 2008). Thicker active layers and thinning permafrost could provide an early sign of climate change in the alpine zone of Rocky Mountain National Park.

Visualization Website

http://www.mscd.edu/~eas/Janke/GEL_3420/ROMO/Home.htm

The website listed above provides additional detailed information about this study. The website features an interactive map in which information about each site can be explored. A site description, metadata, photographs, and a yearly temperature plot of the data is provided for each location.

References

Boike, J., Hagedorn, B. and Roth, K., 2008. Heat and Water Transfer Processes in Permafrost-Affected Soils: A Review of Field and Modeling-Based Studies for the Arctic and Antarctic, 9th International Conference on Permafrost. Plenary Paper, pp. 149-154.

Haeberli, W., 1985. Creep of mountain permafrost: internal structure and flow of alpine rock glaciers. Mitt. der Vers. für Wasserbau, Hydrol. und Glaziologie, 77: 142.

Hauck, C. and Vonder Mühll, D., 2003. Inversion and interpretation of two-dimensional geoelectrical measurements for detecting permafrost in mountainous regions. Permafrost and Periglacial Processes, 14: 305-318.

Isaksen, K., Sollid, J.L., Holmlund, P. and Harris, C., 2007. Recent warming of mountain permafrost in Svalbard and Scandinavia. Journal of Geophysical Research-Earth Surface, 112(F2).

Ives, J.D., 1974. Permafrost. In: J.D. Ives and R. Barry (Editors), Arctic and Alpine Environments. Methuen; distributed in the U.S. by Harper & Row Publishers, London [New York], pp. 159-194.

Ives, J.D. and Fahey, B.D., 1971. Permafrost occurrence in the Front Range, Colorado Rocky Mountains, U.S.A. Journal of Glaciology, 10(58): 105-111.
Janke, J.R., 2005a. The Occurrence of Alpine Permafrost in the Front Range of Colorado. Geomorphology, 67(3-4): 375-389.
Janke, J.R., 2005b. Modeling past and future alpine permafrost distribution in the Colorado Front Range. Earth Surface Processes and Landforms, 30(12): 1495-1508.
Lantz, T.C. and Kokelj, S.V., 2008. Increasing rates of retrogressive thaw slump activity in the Mackenzie Delta region, NWT, Canada. Geophysical Research Letters, 35(6).
Leopold, M. et al., 2008. Using geophysical methods to study the shallow subsurface of a sensitive alpine environment, Niwot Ridge, Colorado Front Range, USA. Arctic Antarctic and Alpine Research, 40(3): 519-530.
Outcalt, S.I. and Hinkel, K.M., 1996. Thermally driven sorption, desorption, and moisture migration in the active layer in Central Alaska. Physical Geography, 17: 77-90.
Riseborough, D., Shiklomanov, N., Etzelmuller, B., Gruber, S. and Marchenko, S., 2008. Recent advances in permafrost modelling. Permafrost and Periglacial Processes, 19(2): 137-156.
Schrott, L. and Sass, O., 2008. Application of field geophysics in geomorphology: Advances and limitations exemplified by case studies. Geomorphology, 93(1-2): 55-73.
Vonder Mühll, D., Hauck, C. and Gubler, H., 2002. Mapping of mountain permafrost using geophysical methods. Progress in Physical Geography, 26(4): 643-660.
Williams, P.J. and Smith, M.W., 1989. The Frozen Earth: Fundamentals of Geocryology. Cambridge University Press, New York, 306 pp.

Acknowledgements

Special thanks are given to the National Park Service, in particular Judy Visty and Cheri Yost, for providing financial and administrative support to conduct this project. Their enthusiasm for the helped renew my interest in the discipline. Field and laboratory assistants from Metropolitan State College of Denver helped gather, interpret, and analyze the data for this project. Luke Stucker, Loren Sorber, Jessica Taylor, Paschal Jennings, Tricia Dienstfrei, Craig Dreiling, and the GEL 3420 Soils class were vital to this project. Additional thanks are extended to the Park Service Employees, Ansel and Robert, for their help in the field and transportation to the field sites. Sam Outcalt greatly improved this report by providing his expert interpretation of the temperature data. Thanks again to all for your help and support.